PHYSICAL REVIEW E **95**, 012203 (2017)

Oscillatory pulses and wave trains in a bistable reaction-diffusion system with cross diffusion

Evgeny P. Zemskov,[1,*] Mikhail A. Tsyganov,[2,†] and Werner Horsthemke[3,‡]

[1]*Federal Research Center for Computer Science and Control, Russian Academy of Sciences, Vavilova 40, 119333 Moscow, Russia*

[2]*Institute of Theoretical and Experimental Biophysics, Russian Academy of Sciences, Institutskaya 3, 142290 Pushchino, Moscow Region, Russia*

[3]*Department of Chemistry, Southern Methodist University, Dallas, Texas 75275-0314, USA*

(Received 6 November 2016; published 4 January 2017)

We study waves with exponentially decaying oscillatory tails in a reaction-diffusion system with linear cross diffusion. To be specific, we consider a piecewise linear approximation of the FitzHugh-Nagumo model, also known as the Bonhoeffer-van der Pol model. We focus on two types of traveling waves, namely solitary pulses that correspond to a homoclinic solution, and sequences of pulses or wave trains, i.e., a periodic solution. The effect of cross diffusion on wave profiles and speed of propagation is analyzed. We find the intriguing result that both pulses and wave trains occur in the bistable cross-diffusive FitzHugh-Nagumo system, whereas only fronts exist in the standard bistable system without cross diffusion.

DOI: 10.1103/PhysRevE.95.012203

I. INTRODUCTION

Waves appear in reaction-diffusion systems as a result of the interaction between the nonlinear kinetic terms and the diffusive transport terms [1]. Most studies of reaction-diffusion equations assume that the diffusion matrix is diagonal. In other words, the diffusive flux of any given species is driven only by its own concentration gradient. There are, however, situations where the effect of the concentration gradients of other species in the system cannot be neglected. The diffusion matrix then has a nondiagonal form, and the system is referred to as cross-diffusive. In chemical systems, cross diffusion is encountered, for instance, in strong electrolytes, micelles, and microemulsions [2–4]. Chemotaxis, where cells, bacteria, and other organisms move in response to certain chemicals in their environment, represents another important example of cross diffusion [5–7].

Cross-diffusion reflects the fact that the spatial motion of one species is influenced by the concentration gradient of another species. This mechanism fits naturally into the context of population dynamics and ecological problems [8–11]. Cross-diffusion has frequently been incorporated into predator-prey models, since prey tends to avoid high concentrations of predators, while predators tend to seek out high concentrations of prey [12–17]. Cross-diffusive effects have also been studied in the context of plasma physics [14,18]. Further, excitable media with elastic coupling can be described by a two-variable reaction-diffusion system with a pure cross-diffusion term [19,20].

In chemical systems, thermodynamics requires that the cross-diffusion coefficients for a given species must go to zero as the concentration of that species approaches zero, i.e., the cross-diffusion terms are nonlinear [2,21,22]. This is, of course, not required for systems to which thermodynamics does not apply, and systems with linear cross diffusion, i.e., the cross-diffusion coefficients are constant, have been studied in a variety of contexts [11–13,16,19,20,23–26]. Cross-diffusion coefficients can be positive or negative. Models where the cross-diffusion terms have opposite signs have been extensively investigated in Refs. [16,25,27–29] and correspond to pursuit-evasion in a predator-prey context. It turns out for such situations that the cross-diffusion effects are more pronounced in systems with pure cross diffusion, i.e., the self-diffusion coefficients vanish [16,28,30,31].

The minimal reaction-diffusion system that can display cross diffusion is of course a two-species system. One of the simplest two-variable models is the FitzHugh-Nagumo (FHN) equations [32,33], also known as the Bonhoeffer-van der Pol model [34–36]. It was originally introduced as a simplification of the Hodgkin-Huxley model [37], which describes the propagation of an action potential along nerve fibers. The FHN model has been widely studied to understand wave propagation in excitable (active) media with diffusive coupling. The simplest waves in this model are traveling fronts, a heteroclinic trajectory in the phase plane, connecting two steady states (fixed points) of the system. Such systems are referred to as bistable systems [38]. Other traveling waves, namely solitary pulses (homoclinic solutions) and sequences of pulses or wave trains (periodic solutions) occur in the FHN-system with one fixed point, i.e., the system is excitable or oscillatory [39]. In the spatially one-dimensional case, the wave profiles typically correspond to a curve with monotonic tails. However, the wave profile can also display oscillatory tails [40–44]. The oscillatory fronts have been described in the standard FHN-type model [41] and in the model with cross diffusion [45,46]. Here we study the other possible types of traveling waves with oscillatory tails, namely solitary pulses and periodic wave trains.

The paper is organized as follows. We introduce the FHN model with cross diffusion in Sec. II. In Sec. III we construct the solitary pulses and periodic wave trains with oscillatory tails, and we discuss the origin of the oscillatory tails in Sec. IV. We summarize our results in Sec. V. The mathematical details of the general solutions and fronts with oscillatory tails are collected in the Appendix.

*http://www.researchgate.net/profile/Evgeny_Zemskov
†tsyganov@iteb.ru
‡whorsthe@mail.smu.edu

 ©2017 American Physical Society

II. THE FITZHUGH-NAGUMO MODEL

The FHN model with cross diffusion [16,25,27,28] is described by the reaction-diffusion equations,

$$\frac{\partial u}{\partial t} = u(1-u)(u-a) - v + D_u\frac{\partial^2 u}{\partial x^2} + h_v\frac{\partial^2 v}{\partial x^2}, \quad (2.1a)$$

$$\frac{\partial v}{\partial t} = \varepsilon(u-v) + D_v\frac{\partial^2 v}{\partial x^2} + h_u\frac{\partial^2 u}{\partial x^2}. \quad (2.1b)$$

The positive parameters a and ε are the excitation threshold and the ratio of time scales. The constants $D_{u,v}$ and $h_{u,v}$ are self- and cross-diffusion coefficients, respectively. Thermodynamic considerations do not apply to the system Eq. (2.1). As explained in Ref. [46], the variables u and v do not correspond to densities of reacting and diffusing particles, and consequently they do not have to be nonnegative. The variable u represents the "activator" or potential variable. It corresponds to the potential across the membrane of the nerve fiber in the original application to the Hodgkin-Huxley model. The variable v represents the "inhibitor" or recovery variable. Further, the cross-diffusion coefficients for u and v do not have to vanish as u and v, respectively, go to zero.

To obtain analytical solutions, we employ a piecewise linear approximation for the nonlinear reaction term in the first equation [38,39,47] and consider the case with equal self-diffusion constants, namely $D_u = D_v \equiv D$ and cross-diffusion constants of opposite sign, $h_v \equiv h = -h_u$. We have

$$\frac{\partial u}{\partial t} = -u - v + H(u-a) + D\frac{\partial^2 u}{\partial x^2} + h\frac{\partial^2 v}{\partial x^2}, \quad (2.2a)$$

$$\frac{\partial v}{\partial t} = \varepsilon(u-v) + D\frac{\partial^2 v}{\partial x^2} - h\frac{\partial^2 u}{\partial x^2}, \quad (2.2b)$$

where $H(u-a)$ is the Heaviside function. The excitation threshold a must be $0 < a < 1/2$ for the system to be bistable and $a > 1/2$ for the system to be excitable.

III. CONSTRUCTION OF TRAVELING WAVES IN A PIECEWISE LINEAR MODEL

We look for solutions $u = u(\xi)$ and $v = v(\xi)$ of Eq. (2.2) with the traveling wave coordinate $\xi = x - ct$ and wave speed c. Traveling waves are solutions of the reaction-diffusion equations that propagate in space without change of the wave shape and with constant speed. Traveling solitary pulses and periodic wave trains are built from parts that are obtained by solving the corresponding ordinary differential equations for each part in the piecewise linear approximation of the nonlinear reaction function.

A. Solitary pulses

The pulse solutions in the piecewise linear model consist of three parts, $u_{1,2,3}$ and $v_{1,2,3}$, for the activator and inhibitor variable, respectively. The solutions form a homoclinic trajectory in the phase plane (u,v). The trajectory sets out from a fixed point, or steady state, and returns to that point. The middle pieces, u_2 and v_2, correspond to the peaks of the waves, whereas the edge pieces, or tails, u_1,v_1 and u_3,v_3, represent the growing and decaying parts, respectively. As $\xi \to \pm\infty$, the pulse approaches a constant value, (u^*,v^*), namely a fixed point of the system. The bistable system has two fixed points, and the pulse can start and end at the first fixed point, (0,0), or the second one, (1/2,1/2), as $\xi \to \pm\infty$. In the first case, the boundary conditions for the pulse solutions are as follows:

$$u_1(\xi \to -\infty) = 0, \quad u_3(\xi \to +\infty) = 0, \quad (3.1a)$$

$$v_1(\xi \to -\infty) = 0, \quad v_3(\xi \to +\infty) = 0. \quad (3.1b)$$

Therefore, the pulse solutions read

$$u_1(\xi) = e^{k_+\xi}[A_{11}\cos(l_-\xi) + A_{13}\sin(l_-\xi)], \quad (3.2a)$$

$$u_2(\xi) = e^{k_+\xi}[A_{21}\cos(l_-\xi) + A_{23}\sin(l_-\xi)] + e^{k_-\xi}[A_{22}\cos(l_+\xi) + A_{24}\sin(l_+\xi)] + 1/2, \quad (3.2b)$$

$$u_3(\xi) = e^{k_-\xi}[A_{32}\cos(l_+\xi) + A_{34}\sin(l_+\xi)], \quad (3.2c)$$

for the activator variable, and

$$v_1(\xi) = e^{k_+\xi}[B_{11}\cos(l_-\xi) + B_{13}\sin(l_-\xi)], \quad (3.3a)$$

$$v_2(\xi) = e^{k_+\xi}[B_{21}\cos(l_-\xi) + B_{23}\sin(l_-\xi)] + e^{k_-\xi}[B_{22}\cos(l_+\xi) + B_{24}\sin(l_+\xi)] + 1/2, \quad (3.3b)$$

$$v_3(\xi) = e^{k_-\xi}[B_{32}\cos(l_+\xi) + B_{34}\sin(l_+\xi)], \quad (3.3c)$$

for the inhibitor variable. The quantities $k_\pm$ and $l_\pm$ are defined in the Appendix.

If the pulse starts and ends at the second fixed point, the boundary conditions read

$$u_1(\xi \to -\infty) = 1/2, \quad u_3(\xi \to +\infty) = 1/2, \quad (3.4a)$$

$$v_1(\xi \to -\infty) = 1/2, \quad v_3(\xi \to +\infty) = 1/2, \quad (3.4b)$$

and the shape of the pulse looks like a well, i.e., an inverted pulse. The dynamics of the inverted pulse resembles the behavior of the ordinary standard pulse and we will omit the discussion of this wave.

The three parts of the pulse profile, (3.2) and (3.3), are fitted together using a specific matching procedure. The matching conditions for the pieces $u_n(\xi)$, $v_n(\xi)$, $n = 1,2,3$, and their derivatives $du_n(\xi)/d\xi, dv_n(\xi)/d\xi$ at the two matching points, $\xi = \xi_0$ and $\xi = \xi_0^*$, are as follows [48]:

$$u_1(\xi_0) = u_2(\xi_0), \quad \frac{du_1(\xi_0)}{d\xi} = \frac{du_2(\xi_0)}{d\xi}, \quad (3.5a)$$

$$u_2(\xi_0^*) = u_3(\xi_0^*), \quad \frac{du_2(\xi_0^*)}{d\xi} = \frac{du_3(\xi_0^*)}{d\xi}, \quad (3.5b)$$

$$v_1(\xi_0) = v_2(\xi_0), \quad \frac{dv_1(\xi_0)}{d\xi} = \frac{dv_2(\xi_0)}{d\xi}, \quad (3.5c)$$

$$v_2(\xi_0^*) = v_3(\xi_0^*), \quad \frac{dv_2(\xi_0^*)}{d\xi} = \frac{dv_3(\xi_0^*)}{d\xi}. \quad (3.5d)$$

We know the value of $u(\xi)$ at the matching points and obtain two additional equations,

$$u_1(\xi_0) = u_3(\xi_0^*) = a. \quad (3.6)$$

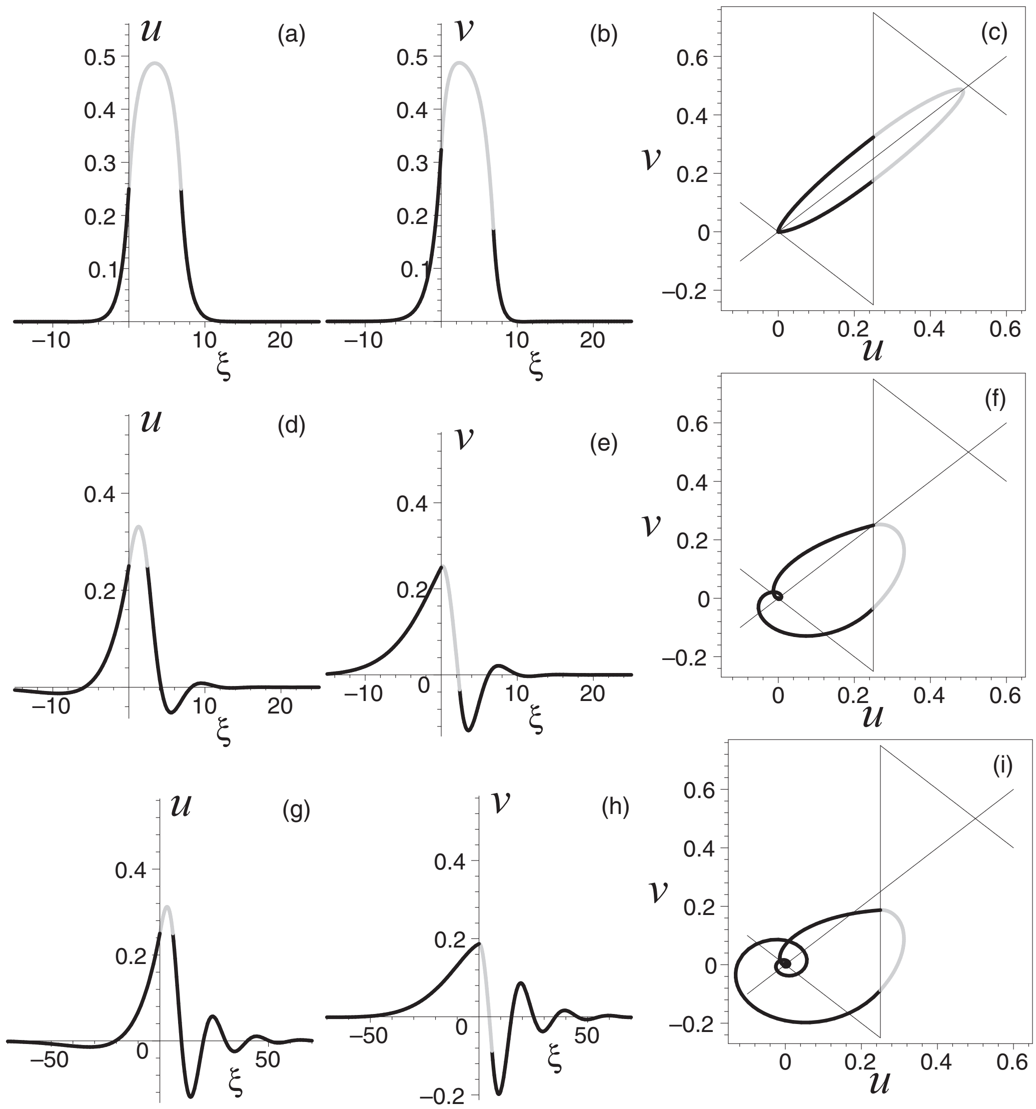

FIG. 1. Solitary pulse profiles for the activator $u(\xi)$ (a, d, g), for the inhibitor $v(\xi)$ (b, e, h), and in the u-v phase plane (bold lines) (c, f, i). The values of the excitation threshold, the ratio of the time scales, and the self-diffusion coefficient are fixed at $a = 1/4$, $\varepsilon = 1$, and $D = 1$, respectively. The middle parts, u_2 and v_2, of the pulses are indicated by the gray color. The null-clines $f(u,v) = -u - v + H(u - a) = 0$ and $g(u,v) = u - v = 0$ are shown by thin lines in panels (c, f, i). Panels (a, b, c) correspond to the case where the self-diffusion and cross-diffusion coefficients are nearly equal: $h = 1.1$. The calculated propagation speed is $c \approx 0.613$. Panels (d, e, f) correspond to the strong cross-diffusion case with $h = 5$, where the calculated speed is $c \approx 4.819$, and panels (g, h, i) to the extra-strong cross-diffusion case with $h = 50$, where the calculated speed is $c \approx 17.846$.

In total, we have 10 equations for 10 unknown constants, $(A_{11}, A_{13}, A_{21}, A_{22}, A_{23}, A_{24}, A_{32}, A_{34}, \xi_0^*, c)$, which allows us to determine the front speed c and the second matching point ξ_0^* uniquely. The first matching point ξ_0 is chosen to be zero due to the translational invariance of the equations, the same choice as in the case of the front solution [45].

The results of the matching procedure, i.e., the profiles of the solitary pulses for the activator and inhibitor variables and in the u-v phase plane are plotted in Fig. 1. The figure shows examples of pulses for three different values of the cross-diffusion constant h. If the value of h is close to the value of the self-diffusion coefficient D, the pulse profile corresponds to a standard ordinary pulse wave of peak-type, the nonoscillatory curve shown in Figs. 1(a)–1(c). If the cross-diffusion effect is strong enough, pronounced oscillations arise in the pulse profile, see Figs. 1(d)–1(f) and Figs. 1(g)–1(i). As shown in Fig. 2, the pulse propagates from left to right, and these oscillations occur in front of the wave peak. This characteristic property of the oscillations in cross-diffusive systems was also found for the front solution [45]. We note here that these oscillations can also occur behind the wave peak, if cross-advection terms are added to the model with cross diffusion [49].

The pulse speed can take both positive and negative values, see Fig. 3, i.e., there exist two counterpropagating pulses for a given value of the cross-diffusion constant h, if h is sufficiently large with respect to D. As the value of h is reduced, the absolute value of the speed decreases, so that at some critical value h_0 there is only a single pulse with $c = 0$. For weaker cross diffusion, no pulse solutions at all exist in the bistable

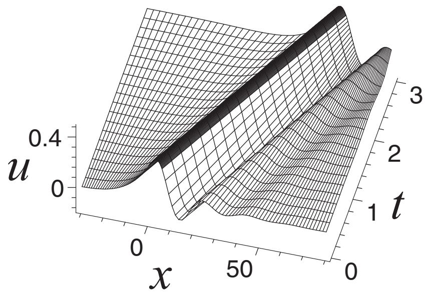

FIG. 2. Space-time plot showing the evolution of the solitary pulse $u(x,t)$ for parameter values from Fig. 1(g), i.e., $a = 1/4$, $\varepsilon = 1$, $D = 1$, and $h = 50$, respectively.

system considered here. Indeed, if the cross-diffusion effect vanishes, the system behaves like the standard FHN system, i.e., pulses exist only in the excitable system, which has only one fixed point.

The results of numerical simulations for pulse propagation are presented in the Supplemental Material [50].

B. Periodic wave trains

The wave train solutions in the piecewise linear model consist of two parts, $u_{1,2}$ and $v_{1,2}$, for the activator and the inhibitor variable, respectively. Since these solutions are periodic, they form a closed smooth trajectory in the phase plane (u,v). This implies that we have again two matching points for the functions and their derivatives. The trajectory sets out from the point $u = a$ at $\xi = \xi_0^0$, passes through this point again at $\xi = \xi_0$, and finally returns to this point at $\xi = \xi_0^*$. Consequently, the period of the wave train is given by $L = \xi_0^* - \xi_0^0$. The matching conditions at the first matching point are the same as for solitary pulses, whereas at the second matching point we need to match two pieces of the solution with different ξ values, namely $(u_1(\xi),v_1(\xi))$ at $\xi = \xi_0^0$ with $(u_2(\xi),v_2(\xi))$ at $\xi = \xi_0^*$. Since the solutions are periodic, there exist no boundary conditions, and the wave train solutions read

$$u_1(\xi) = e^{k_+\xi}[A_{11}\cos(l_-\xi) + A_{13}\sin(l_-\xi)] + e^{k_-\xi}[A_{12}\cos(l_+\xi) + A_{14}\sin(l_+\xi)], \quad (3.7a)$$

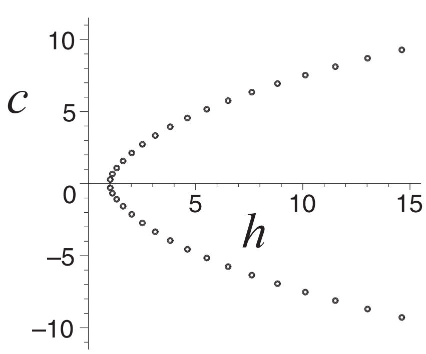

FIG. 3. Speed of the solitary pulse as a function of the cross-diffusion coefficient, $c = c(h)$. The values of the excitation threshold, the ratio of the time scales, and the self-diffusion coefficient are fixed at $a = 1/4$, $\varepsilon = 1$, and $D = 1$, respectively.

$$u_2(\xi) = e^{k_+\xi}[A_{21}\cos(l_-\xi) + A_{23}\sin(l_-\xi)] + e^{k_-\xi}[A_{22}\cos(l_+\xi) + A_{24}\sin(l_+\xi)] + 1/2, \quad (3.7b)$$

for the activator variable, and

$$v_1(\xi) = e^{k_+\xi}[B_{11}\cos(l_-\xi) + B_{13}\sin(l_-\xi)] + e^{k_-\xi}[B_{12}\cos(l_+\xi) + B_{14}\sin(l_+\xi)], \quad (3.8a)$$

$$v_2(\xi) = e^{k_+\xi}[B_{21}\cos(l_-\xi) + B_{23}\sin(l_-\xi)] + e^{k_-\xi}[B_{22}\cos(l_+\xi) + B_{24}\sin(l_+\xi)] + 1/2, \quad (3.8b)$$

for the inhibitor variable. The matching conditions are [48]

$$u_1(\xi_0) = u_2(\xi_0), \quad \frac{du_1(\xi_0)}{d\xi} = \frac{du_2(\xi_0)}{d\xi}, \quad (3.9a)$$

$$u_2(\xi_0^*) = u_1(\xi_0^0), \quad \frac{du_2(\xi_0^*)}{d\xi} = \frac{du_1(\xi_0^0)}{d\xi}, \quad (3.9b)$$

$$v_1(\xi_0) = v_2(\xi_0), \quad \frac{dv_1(\xi_0)}{d\xi} = \frac{dv_2(\xi_0)}{d\xi}, \quad (3.9c)$$

$$v_2(\xi_0^*) = v_1(\xi_0^0), \quad \frac{dv_2(\xi_0^*)}{d\xi} = \frac{dv_1(\xi_0^0)}{d\xi}. \quad (3.9d)$$

As discussed above, the value of u at ξ_0 and ξ_0^* is a:

$$u_1(\xi_0) = u_2(\xi_0^*) = a. \quad (3.10)$$

Again, we have a total of 10 equations for 10 unknown constants, $(A_{11}, A_{12}, A_{13}, A_{14}, A_{21}, A_{22}, A_{23}, A_{24}, \xi_0, c)$, which allows us to determine the front speed c and the first matching point ξ_0 uniquely. The starting point ξ_0^0 is chosen to be zero due to translational invariance of the equations as above. The period of the wave train, $L = \xi_0^* - \xi_0^0$, is now an additional parameter of the solution. The dependence of the speed of the wave train c on the period of the wave train L is known as the dispersion relation. For wave trains with a standard profile, the dispersion relation curves are monotonic [51]. For wave trains that display oscillations in their profile, the dispersion relations are anomalous. This is the situation in our study.

The profiles of periodic wave trains for the activator and inhibitor variables and in the u-v phase plane for fixed values of the cross-diffusion constant h and three values of the period L are shown in Figs. 4 and 5. There exist three types of wave trains, one with a symmetric profile and two with asymmetric profiles. The wave train with a symmetric profile has the matching point ξ_0 at the center of the period. The wave trains with asymmetric profiles have either $\xi_0 < L/2$ or $\xi_0 > L/2$. The asymmetric wave train is localized near one fixed point in the u-v phase plane, whereas the symmetric one visits the vicinity of both fixed points. The speed values of the two asymmetric wave trains coincide and are larger than the speed of the symmetric wave train. Figures 4 and 5 show the asymmetric (fast wave) and symmetric (slow wave) wave trains, respectively. The waves are displayed for one period and for positive values of the speed. If the value of L is small, the waves show standard ordinary behavior, see Figs. 4(a)–4(c) and 5(a)–5(c). If the period is large, then

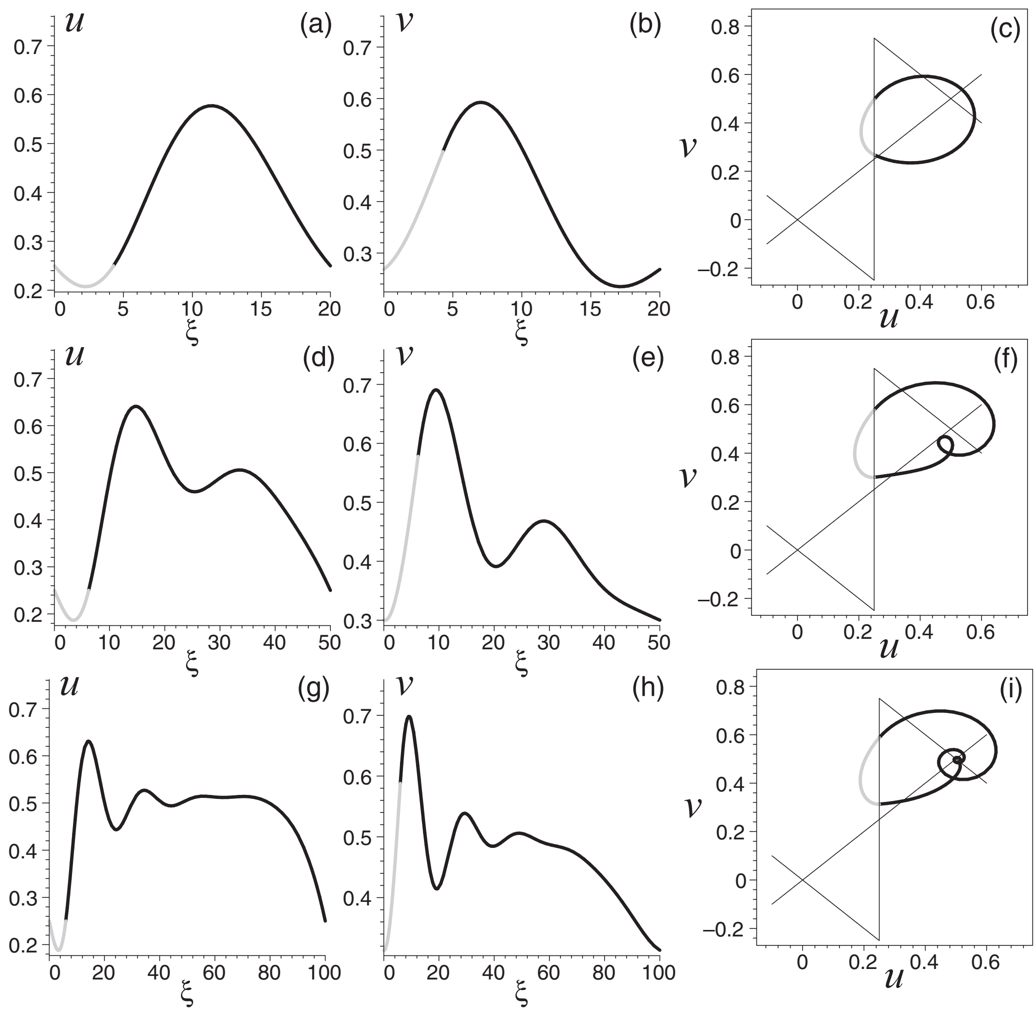

FIG. 4. Periodic wave train (fast wave) profiles for the activator $u(\xi)$ (a, d, g), for the inhibitor $v(\xi)$ (b, e, h), and in the u-v phase plane (bold lines) (c, f, i). The values of the excitation threshold, the ratio of the time scales, and the self- and cross-diffusion coefficients are fixed at $a = 1/4$, $\varepsilon = 1$, $D = 1$, and $h = 50$, respectively. The first parts, u_1 and v_1, of the wave trains are indicated by the gray color. The null-clines $f(u,v) = -u - v + H(u - a) = 0$ and $g(u,v) = u - v = 0$ are shown by thin lines in panels (c, f, i). Panels (a, b, c) correspond to the period $L = 20$, where the calculated speed is $c \approx 19.013$, panels (d, e, f) to $L = 50$, where the calculated speed is $c \approx 17.328$, and panels (g, h, i) to $L = 100$, where the calculated speed is $c \approx 17.851$.

pronounced oscillations appear in the profile, see Figs. 4(g)–4(i) and 5(g)–5(i).

The diagrams for the wave train speed c versus the wave period L, the dispersion relations, are shown in Fig. 6. The results are given for three values of the cross-diffusion constant and for positive values of the speed. For negative values of the speed, the figures are inverted with respect to the $0 - L$ (horizontal) axis. The $c = c(L)$ dependence has the typical property of an anomalous dispersion relation, namely oscillatory behavior, if the value of h is large, see Fig. 6(c).

The results of numerical simulations for dispersion relations are presented in Supplemental Material [50].

IV. DISCUSSION

To understand the origin of the oscillatory waves, it is instructive to compare the interplay of self- and cross-diffusion terms in the model equations. First we consider a two-variable pure diffusion system, where the cross-diffusion terms have the same sign,

$$\frac{\partial u}{\partial t} = D\frac{\partial^2 u}{\partial x^2} + h\frac{\partial^2 v}{\partial x^2}, \tag{4.1a}$$

$$\frac{\partial v}{\partial t} = D\frac{\partial^2 v}{\partial x^2} + h\frac{\partial^2 u}{\partial x^2}. \tag{4.1b}$$

Then we have the following matrix equation, see the Appendix for details,

$$\begin{pmatrix} D\lambda^2 + c\lambda & h\lambda^2 \\ h\lambda^2 & D\lambda^2 + c\lambda \end{pmatrix}\begin{pmatrix} A \\ B \end{pmatrix} = 0, \tag{4.2}$$

and the corresponding characteristic equation is

$$[(D\lambda + c)^2 - h^2\lambda^2]\lambda^2 = 0. \tag{4.3}$$

All eigenvalues $\lambda_{1,2} = 0$ and $\lambda_{3,4} = -c/(D \pm h)$ are real, and the solutions have the usual exponential terms, i.e., there are

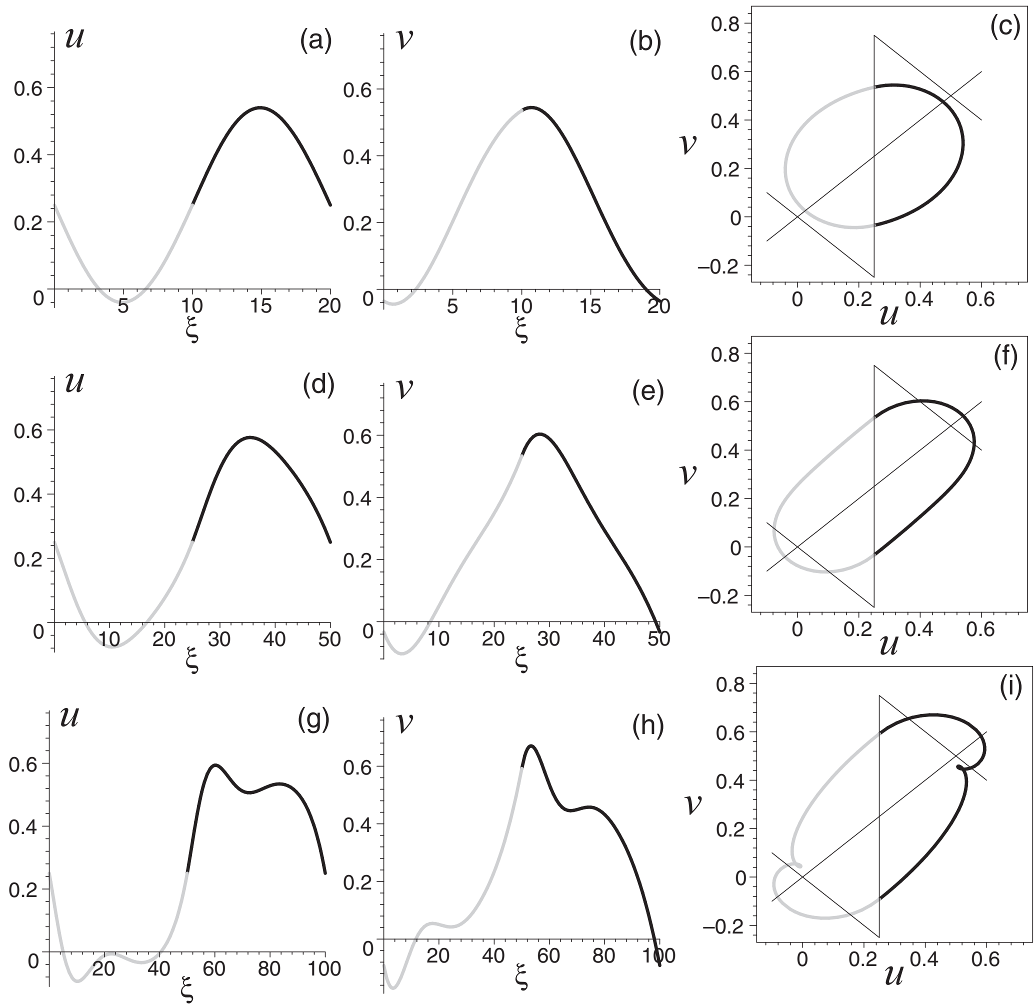

FIG. 5. Periodic wave train (slow wave) profiles for the activator $u(\xi)$ (a, d, g), the inhibitor $v(\xi)$ (b, e, h), and in the u-v phase plane (bold lines) (c, f, i). The values of the excitation threshold, the ratio of the time scales, and the self- and cross-diffusion coefficients are fixed at $a = 1/4$, $\varepsilon = 1$, $D = 1$, and $h = 50$, respectively. The first parts, u_1 and v_1, of the wave trains are indicated by the gray color. The null-clines $f(u,v) = -u - v + H(u - a) = 0$ and $g(u,v) = u - v = 0$ are shown by thin lines in panels (c, f, i). Panels (a, b, c) correspond to the period $L = 20$, where the calculated speed is $c \approx 18.595$, panels (d, e, f) to $L = 50$, where the calculated speed is $c \approx 12.551$, and panels (g, h, i) to $L = 100$, where the calculated speed is $c \approx 13.780$.

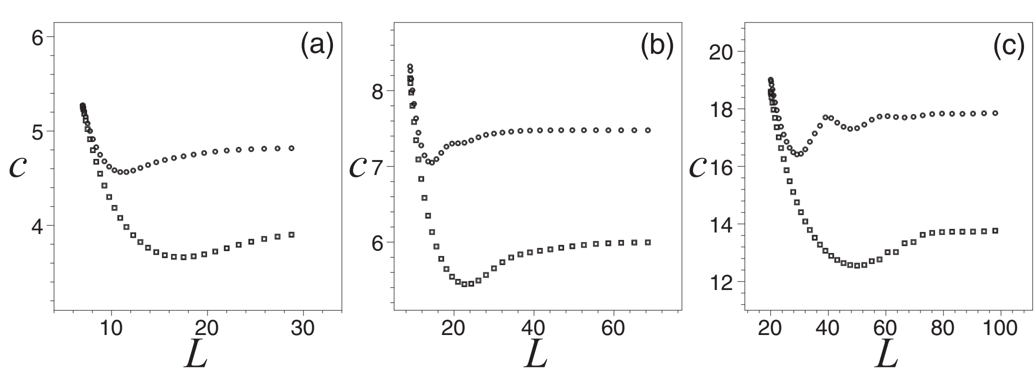

FIG. 6. Speed of the periodic wave train as a function of the period (dispersion relation), $c = c(L)$, for (a) $h = 5$, (b) $h = 10$, and (c) $h = 50$. Wave trains with asymmetric and symmetric profiles are marked by circles and squares, respectively. The values of the excitation threshold, the ratio of the time scales, and the self-diffusion coefficient are fixed at $a = 1/4$, $\varepsilon = 1$, and $D = 1$, respectively.

no oscillations in the wave profiles. However, if the cross-diffusion terms have the opposite sign,

$$\frac{\partial u}{\partial t} = D\frac{\partial^2 u}{\partial x^2} + h\frac{\partial^2 v}{\partial x^2}, \tag{4.4a}$$

$$\frac{\partial v}{\partial t} = D\frac{\partial^2 v}{\partial x^2} - h\frac{\partial^2 u}{\partial x^2}, \tag{4.4b}$$

the characteristic equation,

$$[(D\lambda + c)^2 + h^2\lambda^2]\lambda^2 = 0, \tag{4.5}$$

yields two complex eigenvalues, $\lambda_{3,4} = -c/(D \pm ih)$, and the solutions have cosine and sine terms, i.e., oscillations appear in the wave profiles.

Next we include a piecewise linear reaction term in the pure cross-diffusive system,

$$\frac{\partial u}{\partial t} = -v + H(u-a) + h\frac{\partial^2 v}{\partial x^2}, \tag{4.6a}$$

$$\frac{\partial v}{\partial t} = u \pm h\frac{\partial^2 u}{\partial x^2}. \tag{4.6b}$$

If the cross-diffusion terms are of same signs, the plus sign in Eq. (4.6b), the characteristic equation reads

$$h^2\lambda^4 - c^2\lambda^2 - 1 = 0. \tag{4.7}$$

Two eigenvalues,

$$\lambda^2 = \frac{1}{2h^2}(c^2 + \sqrt{c^4 + 4h^2}), \tag{4.8}$$

are real, and two other,

$$\lambda^2 = \frac{1}{2h^2}(c^2 - \sqrt{c^4 + 4h^2}), \tag{4.9}$$

are imaginary. If the model equations have cross-diffusion terms with opposite signs, the minus sign in Eq. (4.6b), the characteristic equation,

$$(h\lambda^2 - 1)^2 + c^2\lambda^2 = 0, \tag{4.10}$$

produces all complex eigenvalues as above.

Thus, cross-diffusive terms with opposite signs are crucial for the existence of the traveling waves with oscillatory tails.

V. SUMMARY

We wish to emphasize the main result of this work, namely that solitary pulses and periodic wave trains exist in the *bistable* reaction-diffusion FHN system with cross diffusion, whereas fronts are the ordinary solutions in FHN-type bistable systems without cross diffusion [38]. This result was also obtained for a particular case [31], namely a FHN-type system with pure cross diffusion, $D = 0$. In conclusion, fronts, pulses, and wave trains can occur simultaneously in the FHN system with the same set of values for the model parameters, i.e., a, ε, D, and h. We have also shown that sufficiently strong cross-diffusion leads to oscillations in the profile of the pulse and wave train solutions. We have found further that the dispersion relation for the wave trains displays anomalous behavior, i.e., it is nonmonotonic, if the cross-diffusion coefficients are large compared to the self-diffusion coefficients. Our results show that cross diffusion can have nontrivial effects and change qualitatively the spatiotemporal dynamics of reaction-diffusion systems.

ACKNOWLEDGMENTS

The authors thank Vadim N. Biktashev for useful discussion.

APPENDIX: ANALYTICAL SOLUTIONS FOR FRONTS WITH OSCILLATORY TAILS [45]

We consider the case with $\varepsilon = 1$. Then the model equations for traveling waves $u = u(\xi)$ and $v = v(\xi)$, where $\xi = x - ct$ is the traveling wave coordinate and c is the wave propagation speed, are

$$D\frac{d^2u}{d\xi^2} + h\frac{d^2v}{d\xi^2} + c\frac{du}{d\xi} - u - v + H(u-a) = 0, \tag{A1a}$$

$$D\frac{d^2v}{d\xi^2} - h\frac{d^2u}{d\xi^2} + c\frac{dv}{d\xi} + u - v = 0. \tag{A1b}$$

The general solutions have the form

$$u(\xi) = \sum_{n=1}^{4} A_n e^{\lambda_n \xi} + u^*, \tag{A2a}$$

$$v(\xi) = \sum_{n=1}^{4} B_n e^{\lambda_n \xi} + v^*, \tag{A2b}$$

where A_n, B_n, u^*, and v^* are constants to be determined in each of the regions $u < a$ and $u > a$.

Substituting the general solutions Eq. (A2) into the model Eq. (A1), we obtain the following matrix equation:

$$\begin{pmatrix} D\lambda^2 + c\lambda - 1 & h\lambda^2 - 1 \\ -h\lambda^2 + 1 & D\lambda^2 + c\lambda - 1 \end{pmatrix}\begin{pmatrix} A \\ B \end{pmatrix} = 0. \tag{A3}$$

The characteristic equation reads

$$(D\lambda^2 + c\lambda - 1)^2 - i^2(h\lambda^2 - 1)^2 = 0, \tag{A4}$$

with $i^2 = -1$, and yields four eigenvalues,

$$\lambda_{1,2} = -p - iq \pm \sqrt{b + id} = -p - iq \pm y \pm iz, \tag{A5a}$$

$$\lambda_{3,4} = -p + iq \pm \sqrt{b - id} = -p + iq \pm y \mp iz, \tag{A5b}$$

where

$$p = \frac{cD}{2(D^2 + h^2)}, \quad q = \frac{ch}{2(D^2 + h^2)}, \tag{A6a}$$

$$b = p^2 - q^2 + \frac{p+q}{c/2}, \quad d = 2pq - \frac{p-q}{c/2}, \tag{A6b}$$

$$y = \sqrt{(\sqrt{b^2 + d^2} + b)/2}, \tag{A6c}$$

$$z = \sqrt{(\sqrt{b^2 + d^2} - b)/2}. \tag{A6d}$$

Then the general solutions become

$$u(\xi) = e^{k_+\xi}[A_1\cos(l_-\xi) + A_3\sin(l_-\xi)] + e^{k_-\xi}[A_2\cos(l_+\xi) + A_4\sin(l_+\xi)] + u^*, \quad \text{(A7a)}$$

$$v(\xi) = e^{k_+\xi}[B_1\cos(l_-\xi) + B_3\sin(l_-\xi)] + e^{k_-\xi}[B_2\cos(l_+\xi) + B_4\sin(l_+\xi)] + v^*, \quad \text{(A7b)}$$

where $k_\pm = \pm y - p$ and $l_\pm = z \pm q$, respectively.

The integration constants B are expressed as

$$B_{1,3} = -\frac{1}{\gamma_1^2+\delta_1^2}[(\alpha_1\gamma_1+\beta_1\delta_1)A_{1,3} \mp (\alpha_1\delta_1-\beta_1\gamma_1)A_{3,1}], \quad \text{(A8a)}$$

$$B_{2,4} = -\frac{1}{\gamma_2^2+\delta_2^2}[(\alpha_2\gamma_2+\beta_2\delta_2)A_{2,4} \mp (\alpha_2\delta_2-\beta_2\gamma_2)A_{4,2}], \quad \text{(A8b)}$$

with

$$\alpha_1 = D(k_+^2 - l_-^2) + ck_+ - 1, \quad \beta_1 = l_-(2Dk_+ + c), \quad \text{(A9a)}$$

$$\gamma_1 = h(k_+^2 - l_-^2) - 1, \quad \delta_1 = 2hk_+l_-, \quad \text{(A9b)}$$

$$\alpha_2 = D(k_-^2 - l_+^2) + ck_- - 1, \quad \beta_2 = l_+(2Dk_- + c), \quad \text{(A9c)}$$

$$\gamma_2 = h(k_-^2 - l_+^2) - 1, \quad \delta_2 = 2hk_-l_+. \quad \text{(A9d)}$$

Front solutions consist of two tails that approach the corresponding fixed points as $\xi \to \pm\infty$. The boundary conditions for the front solutions are

$$u_1(\xi \to -\infty) = 0, \quad u_2(\xi \to +\infty) = 1/2, \quad \text{(A10a)}$$

$$v_1(\xi \to -\infty) = 0, \quad v_2(\xi \to +\infty) = 1/2. \quad \text{(A10b)}$$

Therefore, the front solutions read

$$u_1(\xi) = e^{k_+\xi}[A_{11}\cos(l_-\xi) + A_{13}\sin(l_-\xi)], \quad \text{(A11a)}$$

$$u_2(\xi) = e^{k_-\xi}[A_{22}\cos(l_+\xi) + A_{24}\sin(l_+\xi)] + 1/2, \quad \text{(A11b)}$$

$$v_1(\xi) = e^{k_+\xi}[B_{11}\cos(l_-\xi) + B_{13}\sin(l_-\xi)], \quad \text{(A11c)}$$

$$v_2(\xi) = e^{k_-\xi}[B_{22}\cos(l_+\xi) + B_{24}\sin(l_+\xi)] + 1/2. \quad \text{(A11d)}$$

In fact, the integration constants A_{mn} and B_{mn} ($m = 1,2$ and $n = 1,\ldots,4$) are the same as A_n and B_n; the subscript m is introduced only to differentiate between the first and the second tail of the front solution.

The matching conditions at the matching point ξ_0 are

$$u_1(\xi_0) = u_2(\xi_0), \quad \frac{du_1(\xi_0)}{d\xi} = \frac{du_2(\xi_0)}{d\xi}, \quad \text{(A12a)}$$

$$v_1(\xi_0) = v_2(\xi_0), \quad \frac{dv_1(\xi_0)}{d\xi} = \frac{dv_2(\xi_0)}{d\xi}. \quad \text{(A12b)}$$

There is one additional equation, namely $u_1(\xi_0) = a$. We have five equations for five unknown constants, $(A_{11}, A_{13}, A_{22}, A_{24}, c)$, and the front speed c may be determined uniquely.

[1] V. Méndez, S. Fedotov, and W. Horsthemke, *Reaction-Transport Systems* (Springer, Heidelberg, 2010).
[2] Vladimir K. Vanag and Irving R. Epstein, Cross-diffusion and pattern formation in reaction-diffusion systems, Phys. Chem. Chem. Phys. **11**, 897 (2009).
[3] Vladimir K. Vanag, Federico Rossi, Alexander Cherkashin, and Irving R. Epstein, Cross-diffusion in a water-in-oil microemulsion loaded with malonic acid or ferroin. Taylor dispersion method for four-component systems, J. Phys. Chem. B **112**, 9058 (2008).
[4] Federico Rossi, Vladimir K. Vanag, Enzo Tiezzi, and Irving R. Epstein, Quaternary cross diffusion in water-in-oil microemulsions loaded with a component of the Belousov–Zhabotinsky reaction, J. Phys. Chem. B **114**, 8140 (2010).
[5] D. Lauffenburger, R. Aris, and K. Keller, Effects of cell motility and chemotaxis on microbial population growth, Biophys. J. **40**, 209 (1982).
[6] Elena O. Budrene and Howard C. Berg, Dynamics of formation of symmetrical patterns by chemotactic bacteria, Nature **376**, 49 (1995).
[7] Le Dung, On a time-dependent bio-reactor model with chemotaxis, Appl. Math. Comput. **131**, 531 (2002).
[8] N. Shigesada, K. Kawasaki, and E. Teramoto, Spatial segregation of interacting species, J. Theor. Biol. **79**, 83 (1979).
[9] Yu. A. Kuznetsov, M. Ya. Antonovsky, V. N. Biktashev, and E. A. Aponina, A cross-diffusion model of forest boundary dynamics, J. Math. Biol. **32**, 219 (1994).
[10] F. S. Berezovskaya and G. P. Karev, Bifurcations of traveling waves in population taxis models, Phys. Uspekhi **42**, 917 (1999).
[11] A. Okubo and S. A. Levin, *Diffusion and Ecological Problems* (Springer-Verlag, New York, 2001).
[12] Edward Kerner, Further considerations on the statistical mechanics of biological associations, Bull. Math. Biophys. **21**, 217 (1959).
[13] Jacob Jorné, The diffusive Lotka-Volterra oscillating system, J. Theor. Biol. **65**, 133 (1977).
[14] D. del Castillo-Negrete, B. A. Carreras, and V. Lynch, Front propagation and segregation in a reaction-diffusion model with cross-diffusion, Physica D **168-169**, 45 (2002).
[15] M. A. Tsyganov, J. Brindley, A. V. Holden, and V. N. Biktashev, Soliton-like phenomena in one-dimensional cross-diffusion systems: A predator-prey pursuit and evasion example, Physica D **197**, 18 (2004).
[16] V. N. Biktashev and M. A. Tsyganov, Solitary waves in excitable systems with cross-diffusion, Proc. Royal Soc. A **461**, 3711 (2005).
[17] J. Brindley, V. H. Biktashev, and M. A. Tsyganov, Invasion waves in populations with excitable dynamics, Biol. Invasions **7**, 807 (2005).
[18] D. del Castillo-Negrete and B. A. Carreras, Stratified shear flows in a model of turbulence-shear flow interaction, Phys. Plasmas **9**, 118 (2002).
[19] Julyan H. E. Cartwright, E. Hernández-García, and Oreste Piro, Burridge-Knopoff Models as Elastic Excitable Media, Phys. Rev. Lett. **79**, 527 (1997).

[20] Julyan H. E. Cartwright, Víctor M. Eguíluz, Emilio Hernández-García, and Oreste Piro, Dynamics of elastic excitable media, Int. J. Bif. Chaos **09**, 2197 (1999).
[21] N. Kumar and W. Horsthemke, Effects of cross diffusion on Turing bifurcations in two-species reaction-transport systems, Phys. Rev. E **83**, 036105 (2011).
[22] G. Gambino, M. C. Lombardo, and M. Sammartino, Turing instability and traveling fronts for a nonlinear reaction–diffusion system with cross-diffusion, Math. Comp. Simulation **82**, 1112 (2012).
[23] I. Berenstein and C. Beta, Cross-diffusion in the two-variable Oregonator model, Chaos **23**, 033119 (2013).
[24] A. Madzvamuse and R. Barreira, Exhibiting cross-diffusion-induced patterns for reaction-diffusion systems on evolving domains and surfaces, Phys. Rev. E **90**, 043307 (2014).
[25] M. A. Tsyganov and V. N. Biktashev, Classification of wave regimes in excitable systems with linear cross diffusion, Phys. Rev. E **90**, 062912 (2014).
[26] G. Gambino, M. C. Lombardo, S. Lupo, and M. Sammartino, Super-critical and sub-critical bifurcations in a reaction-diffusion Schnakenberg model with linear cross-diffusion, Ricerche di Matematica **65**, 449 (2016).
[27] M. A. Tsyganov, J. Brindley, A. V. Holden, and V. N. Biktashev, Quasisoliton Interaction of Pursuit-Evasion Waves in a Predator-Prey System, Phys. Rev. Lett. **91**, 218102 (2003).
[28] V. N. Biktashev and M. A. Tsyganov, Envelope Quasisolitons in Dissipative Systems with Cross-Diffusion, Phys. Rev. Lett. **107**, 134101 (2011).
[29] M. A. Budroni, Cross-diffusion-driven hydrodynamic instabilities in a double-layer system: General classification and nonlinear simulations, Phys. Rev. E **92**, 063007 (2015).
[30] E. P. Zemskov and A. Yu. Loskutov, Oscillatory traveling waves in excitable media, J. Exper. Theor. Phys. **107**, 344 (2008).
[31] E. P. Zemskov, I. R. Epstein, and A. Muntean, Oscillatory pulses in FitzHugh–Nagumo type systems with cross-diffusion, Math. Med. Biol. **28**, 217 (2011).
[32] R. FitzHugh, Impulses and physiological states in theoretical models of nerve membrane, Biophys. J. **1**, 445 (1961).
[33] J. Nagumo, S. Arimoto, and S. Yoshizawa, An active pulse transmission line simulating nerve axon, Proc. IRE **50**, 2061 (1962).
[34] B. van der Pol, On relaxation-oscillations, Phil. Mag. **2**, 978 (1926).
[35] K. F. Bonhoeffer, Über die Aktivierung von Passivem Eisen in Salpetersäure, Z. Elektrochem. **47**, 147 (1941).
[36] K. F. Bonhoeffer, Activation of passive iron as a model for the excitation of nerve, J. Gen. Physiol. **32**, 69 (1948).
[37] A. L. Hodgkin and A. F. Huxley, A quantitative description of membrane current and its application to conduction and excitation in nerve, J. Physiol. **117**, 500 (1952).
[38] J. Rinzel and D. Terman, Propagation phenomena in a bistable reaction-diffusion system, SIAM J. Appl. Math. **42**, 1111 (1982).
[39] J. Rinzel and J. B. Keller, Traveling wave solutions of a nerve conduction equation, Biophys. J. **13**, 1313 (1973).
[40] K. K. Manne, A. J. Hurd, and V. M. Kenkre, Nonlinear waves in reaction-diffusion systems: The effect of transport memory, Phys. Rev. E **61**, 4177 (2000).
[41] E. P. Zemskov, V. S. Zykov, K. Kassner, and S. C. Müller, Analytic solutions for monotonic and oscillating fronts in a reaction-diffusion system under external fields, Physica D **183**, 117 (2003).
[42] P. Carter and B. Sandstede, Fast pulses with oscillatory tails in the FitzHugh-Nagumo system, SIAM J. Math. Anal. **47**, 3393 (2015).
[43] P. Carter, B. de Rijk, and B. Sandstede, Stability of traveling pulses with oscillatory tails in the FitzHugh-Nagumo system, J. Nonlin. Sci. **26**, 1369 (2016).
[44] Paul A. Carter, Fast Pulses with Oscillatory Tails in the FitzHugh-Nagumo System, Ph.D. thesis, Brown University, Providence, RI (2016).
[45] E. P. Zemskov, K. Kassner, and M. J. B. Hauser, Wavy fronts and speed bifurcation in excitable systems with cross diffusion, Phys. Rev. E **77**, 036219 (2008).
[46] E. P. Zemskov, M. A. Tsyganov, and W. Horsthemke, Wavy fronts in a hyperbolic FitzHugh-Nagumo system and the effects of cross diffusion, Phys. Rev. E **91**, 062917 (2015).
[47] H. P. McKean, Nagumo's equation, Adv. Math. **4**, 209 (1970).
[48] E. P. Zemskov and A. Yu. Loskutov, Traveling waves in a piecewise-linear reaction-diffusion model of excitable medium, Biophysics **54**, 631 (2009).
[49] E. P. Zemskov, K. Kassner, M. A. Tsyganov, and M. J. B. Hauser, Wavy fronts in reaction-diffusion systems with cross advection, Eur. Phys. J. B **72**, 457 (2009).
[50] See Supplemental Material at http://link.aps.org/supplemental/10.1103/PhysRevE.95.012203 for numerical simulations of wave propagation.
[51] M. A. Tsyganov, V. N. Biktashev, and G. R. Ivanitsky, Negative refractoriness in excitable systems with cross-diffusion, Biophysics **54**, 513 (2009).